BUILDING EXTRACTION USING LIDAR DEMS AND IKONOS IMAGES

G. Sohn, I. Dowman

Dept. of Geomatic Engineering, University College London, Gower Street, London, WC1E 6BT UK – (gsohn, idowman)@ge.ucl.ac.uk

Commission III, WG III/3

KEY WORDS: LIDAR, IKONOS, Automation, DEM/DTM, Filtering

ABSTRACT:

An automated method for boundary representation of building objects has been considered as a core processor for 3D city modelling. Since the reconstruction of generic building shape fundamentally depends on geometric features extracted from data sources, it suffers difficulties especially when a monocular imagery with high scene complexity is solely used. The research described in this paper aims to develop an automated method for building extraction, in which individual building object is localized and boundaries of polyhedral building shape are delineated with a less specific building model. The developed technique focuses on an exploitation of synergy of Ikonos imagery combined with a LIDAR DEM. Individual buildings are localized with rectangle polygon by a hierarchical segmentation of LIDAR DEM and Ikonos multi-spectral information. This polygon is recursively partitioned by linear features extracted from Ikonos image and LIDAR space, which results in a set of convex polygons. Only polygons comprising "significant" parts of building shape are verified and aggregated. Finally, polyhedral building shapes are reconstructed. Several results are presented with a discussion of evaluation and limitations of our method.

1. INTRODUCTION

A lot of photogrammetry research has been focused on the development of techniques to reconstruct the boundary representation of building objects in high-density urban areas. The automation of this building extraction technique is essential in dealing with the increased demand for 3D city modelling as an efficient method for compilation of building layers, or as a base layer for 3D reconstruction of building models.

In earlier days, most building extraction techniques have relied on 2D feature analysis (Janes et al., 1994; Kim & Muller, 1995; Noronha & Nevatia, 1997), in which straight lines or corners extracted from aerial photographs are perceptually grouped, but the building model targeted is rather strongly constrained to decrease the uncertainty of building hypothesis generation and its verification. For achieving more unconstrained building representation, this technique has been extended to 3D feature analysis using multiple imageries, in which higher density of features belonging to building structure, are generated and grouped; to this end, 3D corners (Fischer et al., 1998), 3D lines (Baillard et, al., 1999a), and 3D planar polygons (Ameri & Fritsch, 2000) were used. Since the aforementioned approaches rely on the reliability and density of features extracted from aerial photographs, these techniques suffer difficulties when extracted features are highly fragmented or missed due to low contrast, occlusion and shadow effects.

Thus, other data sources have been exploited for compensating for the disadvantages of aerial photograph. In this area, LIDAR data, which is acquired by airborne laser scanners, has been used as an attractive alternative to aerial photography due to high vertical accuracy and high point density. As a single source, LIDAR data has been used to reconstruct various types of building shape; parametric model (Mass & Vosselman, 1999; Wang & Schenk, 2000), prismatic model with flat roof (Weidner & Förstner, 1995) and polyhedral building with the restriction on building orientation (Vosselman, 1999). Although LIDAR data have several advantages of building localization and planar patch extraction compared to aerial photographs, there is also drawback to delineate building boundaries with break-lines when LIDAR data is solely used, even with extremely high density of 7 points per square metre (Vosselman, 1999). Therefore, a fusion technique is recommended to combine the complementary nature of the two different data sources for building extraction (Schenk & Csatho, 2002).

The research described in this paper aims to exploit a synergy of single Ikonos satellite imagery with 1-metre resolution, and LIDAR data with 3-metre point spacing. Several aspects are considered in our research; firstly, considering the complexity of high-density urban area, an individual building object is separated from surrounding objects before applying our building extraction algorithm; secondly, because rather coarse resolution datasets are used, the use of LIDAR data is investigated for use when linear features extracted from single Ikonos imagery are not sufficient for building boundary representation; finally, the coarse resolution of LIDAR data used makes it difficult to extract reliable planar roof faces or coplanar grouping of linear features. Thus, a method to delineate a polyhedral building shape by only linear features extracted from the two different datasets is targeted.

Our building extraction method can be categorized into the following sequential processes; (1) a localization of individual buildings is achieved by hierarchical segmentation of LIDAR space combined with Ikonos multi-spectral bands; (2) "intensity" line cues are extracted from Ikonos imagery and then, the verification of boundary lines is made over LIDAR space; (3) "virtual" line cues are generated, in which parallel and "U" structured boundary lines are inferred over LIDAR space from each "intensity" line cue; (4) a polyhedral building shape is reconstructed by a collection of "significant" parts with

polygon geometry, which is obtained by recursive partitioning of individual building blobs with integrated line cues.

In next section, we describe a building localization method, in which individual building objects are bounded with rectangles for further processing. In section three, we describe cue generation and grouping process for the boundary representation of a polyhedral building shape. In section four, some results are presented with a discussion of evaluation and limitations of our method. Finally, we draw conclusions and suggest future research tasks.

2. BUILDING LOCALIZATION

The scene complexity of high-density urban areas degrades interpretation of single objects, which leads to generation of extraneous hypotheses and requires much larger verification evidence. To cope with this problem, a focusing strategy has been proposed by many researches (Brunn & Weidner, 1997; Baillard & Maitre, 1999; Haala, 1994; Weidner & Förstner, 1995), in which individual buildings are separated from other objects. These approaches share a common strategy of hierarchical object localization, in which on-terrain features and off-terrain features are differentiated with the support of high-resolution height information and then, off-terrain features are further classified into tree and building object classes. As a final result, individual buildings are localized with spatial information bounding them.

Sohn and Dowman (2002) developed a LIDAR filtering technique to automatically differentiate on-terrain points from off-terrain ones using irregularly spaced LIDAR data. This technique was developed to make a LIDAR filter to be self-adaptive to various landforms with different slopes. The fundamental idea behind this is to fragment a LIDAR DEM convolved with heterogeneous terrain slopes (see Figure 1 (a)) into a set of homogeneous sub-region, where underlying terrain can be characterized by single slope (see Figure 1 (b)). Once these homogeneous sub-regions are achieved, the separation between on-terrain points and off-terrain points becomes much simpler, as terrain characteristics are uniformly regularized.

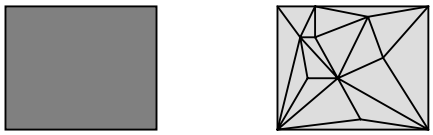

(a) LIDAR DEM (b) fragmented terrain

Figure 1. Illustration of the suggested terrain fragmentation idea; darker grey colour means more different terrain slopes are mixed up in a region.

To realize the aforementioned terrain fragmentation idea, an elementary terrain model is employed for the reconstruction of generic terrain surface. That elementary model is a planar terrain surface (PTS), which is formed in a triangle shape and its three vertices consist of on-terrain points. When a PTS is hypothesized as "real" terrain model over an arbitrary area, several important relationships are defined between PTS and its member points: i) all the member points must be located above PTS ("positive terrain" criterion); ii) member points with less than certain height threshold from PTS are recognized as on-terrain points ("continuity" criterion); iii) the populated on-terrain points over PTS must have the same slope ("homogeneity" criterion). If the PTS satisfies these criteria, its hypothesis as being a planar terrain is verified; otherwise, the most reliable on-terrain point is selected out of its member points and the PTS is fragmented by a Delaunay Triangulation method using the selected on-terrain point. In this way, a LIDAR DEM is recursively fragmented from "coarse" to "fine" scale until all the fragmented segments are verified as PTS. In consequence, the Digital Terrain Model (DTM) is reconstructed by collecting PTSs fragmented at the "finest" scale.

This recursive terrain fragmentation was implemented by a two-step divide-and-conquer triangulation method, in which a LIDAR DEM is fragmented in downward and upward direction. In downward fragmentation, a single PTS is hypothesized as a terrain surface of the entire LIDAR DEM. If this initial plane is not satisfied with the "positive terrain" criterion, the plane is fragmented by selecting a LIDAR point with the minimum distance from the plane and labelling it as on-terrain point. This process continues until all the LIDAR point is located above fragmented PTSs. Then, the upward fragmentation process starts. First, triggering the upward fragmentation for each PTS is determined as investigating whether or not populated on-terrain points have the same slope. If the upward fragmentation is determined over a PTS, three vertices of the PTS and each on-terrain point generated from it are served as constructing a tetrahedron model. Thus, a number of tetrahedron models are generated by all the on-terrain member points and three lateral facet of each tetrahedron are hypothesized as PTS. The "best" tetrahedron model is selected when it leads to a minimum classification error of on- and off-terrain points populated by the model. This model selection was implemented in MDL (Minimum Description Length) framework, where "better" model generates smaller angle dispersions between on-on paired slopes and the tetrahedron model, while bigger angles dispersions between on-off paired slopes and the tetrahedron model. Finally, by selecting the on-terrain member point constructing the "best" tetrahedron model, the PTS is triangulated and thus, fragmented into smaller sub-regions. This process continues until all the PTSs satisfy the "homogeneity" criterion. In consequence, LIDAR points comprising PTSs fragmented at the finest scale are classified into on-terrain points, otherwise, off-terrain labels.

The remaining process for the localization of individual buildings is rather straightforward. For obtaining more reliable off-terrain points only belonging to tree and building objects, outlying points with a height less than a defined threshold from the generated DTM are removed. Then, differentiating building objects from trees is made by the use of Ikonos multi-spectral bands; the normalized difference vegetation indices (NDVI) are computed by a combination of red and near-infrared channels of Ikonos. When LIDAR points are back-projected onto Ikonos image space, a small size of mask is made around them over the NDVI map and a vegetated LIDAR point is detected if a NDVI value larger than a certain threshold is found in the mask. Thus, off-terrain labels are further segmented into building and tree-label class. After a connected component labelling process is applied to irregularly distributed label space, individual building objects are extracted with the boundary information. These building blobs are represented with rectangle polygons, which feedback to recursive partitioning for building extraction.

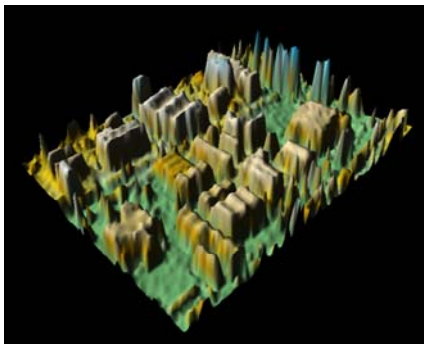

(a) LIDAR DEM

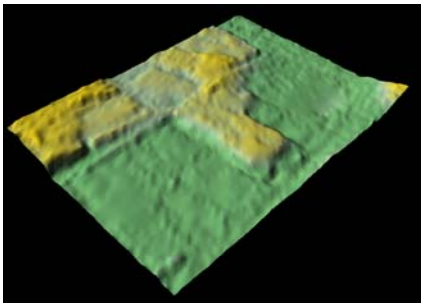

(b) reconstructed DTM

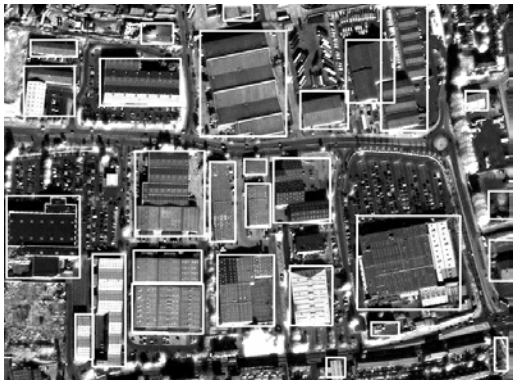

(c) Ikonos imagery overlaid with building blob polygons

Figure 2. Building localization results.

3. BUILDING EXTRACTION

3.1 Intensity line cue generation and filtering

It is assumed that a generic building shape consists of a set of rectilinear lines, but without the limitation of directionality. Thus, as a primary cue for building extraction, straight lines are extracted from Ikonos imagery by the Burns algorithm (Burns et al. 1986). Since extracted line features include a number of extraneous line segments, uncorrelated to building saliencies, it is necessary to filter those distracting features so that only focused lines with significant length located around building boundaries remain. To this end, on-terrain and building-label points classified by our LIDAR filter are used to determine whether or not line primitives can be considered as boundary lines.

First, straight lines extracted by the Burns algorithm are filtered by a length criterion, by which only lines larger than pre-specified length threshold remain for further processing. Then, two rectangle boxes with certain width, l_w, are generated along two orthogonal directions to the line vector filtered in length. The determination of a boundary line can be given if on-terrain and building-label points are simultaneously found in both boxes or if only building-label points are found in one of the boxes and no LIDAR point can be found in the other box. The latter boundary line condition is considered if a low density LIDAR dataset is used.

As a final line filtering process, a geometric disturbance corrupted by noise is regularized over boundary lines. A set of dominant line angles of boundary lines is analysed from a gradient-weighted histogram quantized in 255 discrete angular units. In order to separate a weak, but significant peak from other nearby dominant angles, a hierarchical histogram-clustering method is applied; once the dominant angle, θ_d, is obtained, lines with angle discrepancies are less than certain angel thresholds, θ_{th}, from θ_d are found, and their line geometries are modified as their angles are replaced with θ_d. These modified lines do not contribute to the succeeding dominant angle analysis and the next dominant angle is obtained. In this way, a set of dominant angles is obtained, by which geometric properties of boundary lines can be regularized. Figure 3 shows boundary lines extracted by the support of labelled LIDAR points, after being filtered in length and geometrically regularized in angle, where the length criterion, θ_{th} and l_w are selected as 5-metre, 30º and 5-metre respectively.

(a) extracted straight lines

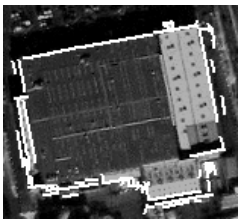

(b) filtered boundary lines

Figure 3. Extracted building boundary lines from Ikonos imagery.

3.2 Virtual line cue generation

Since our research aims to represent a polyhedral building shape by only boundary lines, much larger numbers of line cue need to be obtained than in the case of a parametric building model, it is, however, always a bottle-neck to extract such a cue density due to low contrast, shadow overcast, and occlusion effects, especially when 1-mere satellite imagery of a complex scene is solely used. Thus, virtual line cues are extracted from LIDAR space in order to compensate for the lack of intensity line cue density.

For extracting virtual line cues, the second constraint of polyhedral building shape is assumed that a generic polyhedral building shape is made in some degree of geometric regularity. Based upon this, for each intensity line cue, parallel and "U" structured boundary lines are inferred from LIDAR space. Note that the assumption of geometric regularity is used as a weak constraint in our building extraction process since the geometry

of a polyhedral building may not have any symmetric property. That is, only a portion of virtual cues could be involved to recover significant boundary segments missed in intensity line cue generation. It is, however, subject to the degree of complexity of individual buildings as to what percentage of virtual lines cue can be used. Therefore, a verification process of virtual line cues is necessary. In our method, it will be automatically determined at a higher level of cue generation, namely polygon cue generation, whether or not a virtual line cue should be used in boundary representation of polyhedral building shape.

The process aims to acquire at most three virtual lines starting from an intensity line cue, but it could fail to generate any virtual line cue. The main idea of virtual line detection is that a small virtual box is generated from each intensity line and it grows over building roof so that building-label points are maximally captured without including any on-terrain point. First, a box growing direction, pointing to the location of parallel boundary line, is determined from the selected intensity line. To that direction, a small virtual box is generated and grows until it comes across any on-terrain point. Then, it de-grows in order to have maximum building-label points while in its minimum size (see Figure 4 (a)). In this way, the virtual box is expanded, but at this time, towards to two orthogonal directions to the parallel boundary line detected (see Figure 4 (b)). Thus, "U" structured boundary lines made with the parallel boundary line can be detected. Finally, these three virtual lines detected are back-projected onto image space and then, their line geometry is adjusted by gradient weighted least-square method (see Figure 4 (c)).

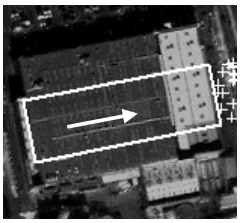
(a) parallel line detection

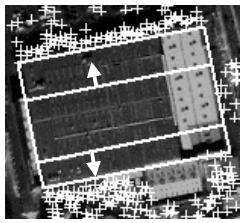
(b) "U" structure line detection

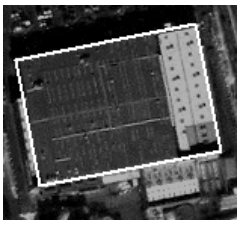
(c) gradient fitted virtual lines

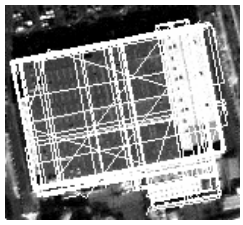
(d) entire virtual lines detected

Figure 4. Results of virtual line cue generation; white lines represents detected virtual lines, white arrow points to the virtual box growing direction and white cross represents on-terrain points.

3.3 Polygon cue generation and grouping

Once "intensity" line and "virtual" lines are extracted, a set of convex polygons is generated by a recursive intersection of both lines. Only the polygons comprising "significant" parts of building shape are verified as "building" polygon. The boundary representation of polyhedral building shape is reconstructed by a collection of "building" polygons. To this end, a line cue grouping process to generate polygon cues was implemented by a Binary Space Partitioning (BSP) method (Fuchs, Kedem & Naylor 1980). Sohn and Dowman (2001) exploited the feasibility of BSP method for building extraction, where polygon cue generation and grouping process rely on straight lines extracted from monocular Ikonos imagery. We expanded this method with a different strategy considering the contribution of LIDAR data.

The BSP is an efficient method to aid recursive partitioning of a region by hyperlines in 2D image space. Figure 5 illustrates this. Suppose that we have an initial polygon with rectangle geometry, P^0, wherein LIDAR points are distributed with on- and building-label (see Figure 5 (a)). This polygon is generated from the previously mentioned building localization process, by which an individual building object is surrounded. For recursive partitioning, a set of hyperlines, $\{h^i: i=1, \ldots, N\}$ are prepared, which are computed as P^0 is intersected respectively by integrated line segments $\{l^i: i=1, \ldots, N\}$ including intensity and virtual line cues. After setting up the hyperline list, all the hyperlines are tested to obtain the "best" partition of P^0 and a hyperline, h^0, with the highest partitioning score is selected to partition the whole LIDAR domain, P^0. For the selection of h^0, a hyperline candidate, h^i, is sequentially selected from the hyperline list, by which P^0 is divided into the positive and negative planes, i.e., P^{0+} and P^{0-}, reflecting whether the dot product of each vertex point of P^0 with h^0 is negative or positive. Then, a normalized cost function, H, computes a partitioning score, which can be given according to a bias degree of label distribution over P^{0+} and P^{0-} partitioned by h^i; if a more biased label distribution is generated, higher score is given. This scoring function, H can be described as follows:

$$H\left(P^0;h^i,l^i\right)=\arg\max\left(H\left(P^{0+};h^i,l^i\right),H\left(P^{0-};h^i,l^i\right)\right) \tag{1}$$

where, scores for P^{0+} and P^{0-} can be obtained respectively by H as follows:

$$\begin{aligned} H\left(P^{0+};h^i,l^i\right)&=\frac{1}{2}\left\{\frac{N_{bld}\left(P^{0+};h^i,l^i\right)}{N_{bld}\left(P^0;h^i,l^i\right)}+\frac{N_{on}\left(P^{0-};h^i,l^i\right)}{N_{on}\left(P^0;h^i,l^i\right)}\right\}\\ H\left(P^{0-};h^i,l^i\right)&=\frac{1}{2}\left\{\frac{N_{bld}\left(P^{0-};h^i,l^i\right)}{N_{bld}\left(P^0;h^i,l^i\right)}+\frac{N_{on}\left(P^{0+};h^i,l^i\right)}{N_{on}\left(P^0;h^i,l^i\right)}\right\}\end{aligned} \tag{2}$$

In Equation 2, N_{on} and N_{bld} are functions to count numbers of on-terrain or building-label points belonging to a corresponding polygon. Likely to the case of h^i, the partitioning scores for remaining hyperlines are measured by H. Finally, a hyperline with maximum score is selected as h^0 to partition P^0 and geometric information of P^0 and h^0 are stored as a root node of BSP tree for further recursive partitioning (see Figure 5 (b)). The same method used for the partition of P^0 is applied to P^{0+} and P^{0-} respectively, but to only an "open" polygon, which consists of mixed labels, that is on-terrain and building-label and the BSP tree is expanded if new child polygons are generated by the hyperline list (see Figure 5 (c)). This process continues until no leaf node of the BSP tree can be generated.

There are two aspects to considering when the "best" partition of arbitrary polygon is determined. Firstly, due to low point density, a "closed" polygon, P^i, which consists of only a building-label, is "earlier" terminated as the final leaf of the BSP tree, though it needs to be divided more. Thus, P^i with point spacing less than expected, i.e., d_{th}, is also tested to look for the "best" partition, even if it is closed. In this case, only when either of P^{i+} and P^{i-} is recognized as an "empty" polygon that does not include any point, the partitioning score is given by an area ratio of "empty" polygon over P^i, otherwise the null value is assigned. Thus, the "best" partition of P^i with low point spacing less than d_{th} is determined when P^i is partitioned with the largest "empty" polygon. Secondly, it is necessary to prevent our partitioning method from generating an ignorable building part; if any lateral length or area of resulting child polygon is less than a certain threshold, i.e., l_{th} and a_{th} respectively, its partitioning score is assigned with null value.

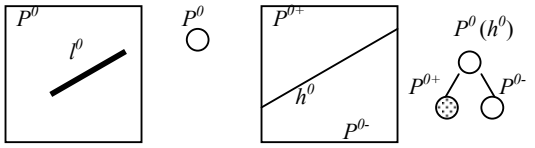

(a) polygon initialisation (b) first BSP partitioning

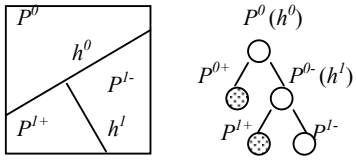

(c) recursive polygon partitioning and BSP tree

Fig. 5: BSP tree construction. In the BSP tree, dot circle and white circle represent "closed" and "open" polygon respectively.

Once a BSP tree is generated, final leaves of the BSP tree are collected. A heuristic filtering is applied to them so that only "building" polygons remain. On the one hand, "open" polygons are investigated whether or not they can be recognized as a building part; if building-label points exist with a significant ratio, i.e., ρ_{th}, it is marked as a "building" polygon. On the other hand, all the "closed" polygons are recognized as "building" parts, but a "closed" polygon is excluded if its member points are less than n_{th} and its expected point spacing is less than $\gamma * d_{th}$, where γ is control parameter.

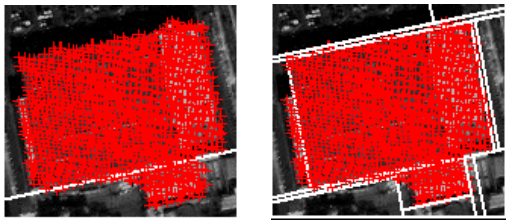

(a) initial partitioning (b) intermediate partitioning

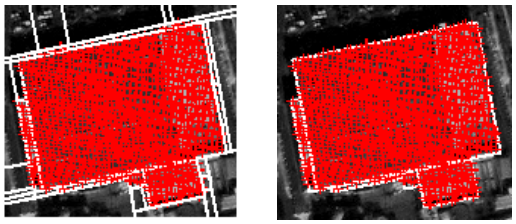

(c) final BSP partitioning (d) after heuristic filtering

Figure 6. Illustration of polygon cue generation and grouping (white line: selected hyperlines, red cross: building-label points).

4. RESULTS

We tested our suggested building extraction technique over a sub-site of Greenwich industrial area in London, which size is 334,125 (m^2). As an image source, Ikonos Precision Pan sharpened imagery with 1-metre resolution was used (see Figure 2 (c)). For the height information, 30,782 LIDAR points were acquired over the test area by OPTEC 1020 airborne laser scanner, which point density is 0.09 (points/m^2), i.e., approximately one point per 3.3 x 3.3 (m^2) (see Figure 2 (a)).

Using the LIDAR DEM of figure 2 (a), the DTM is reconstructed with 15,679 on-terrain points labelled by our LIDAR filter (see Figure 2 (b)), in which three parameters are used; 1-metre height value is chosen as the "continuity" criterion; shape parameters of a sigmoidal function for the "terrain polarity" measurement, i.e., α and β are selected as 0.1 and 45º respectively, which are explained more detail in Sohn and Dowman (2002). For building localization, off-terrain points are further filtered so that the height of remaining points is higher than 4-metre from the reconstructed DTM. When they are projected back onto Ikonos image space, normalized NDVIs are measured within 5x5 neighbouring mask and vegetated off-terrain points are removed if any point with the normalized NDVI larger than 0.8 is found in the mask. The final building localization result is presented in Figure 2 (c), in which 28 buildings with having building-labels larger than 30 points are bounded with rectangle polygons. Note that most residential houses failed to be localised due to the low density of LIDAR data and nearby trees (see bottom right of Figure 2 (c)).

Figure 9 shows the boundary representation result of polyhedral building shapes reconstructed by our building extraction technique. In this result, the boundaries of most building shapes are properly reconstructed by linear features. Although a large amount of erroneous virtual line cues are inferred in each building object, our recursive BSP efficiently prunes distracting linear cues. As a result, in several building objects, we can observe that extended building structures with small size are reconstructed by the contribution of "virtual" line cues even though those parts are occluded or have very low contrast (see Figure 7). Since our recursive part segmentation of polyhedral building shape adopts global-to-fine strategy, building extraction errors are limited to the reconstruction of less "significant" building structures.

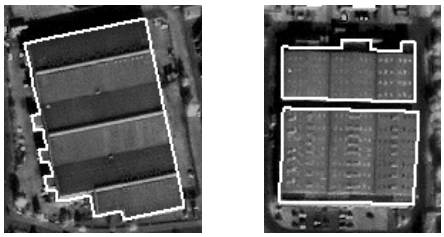

(a) (b)

Figure 7. Building extraction results of (a) small extended and (b) occluded building structures.

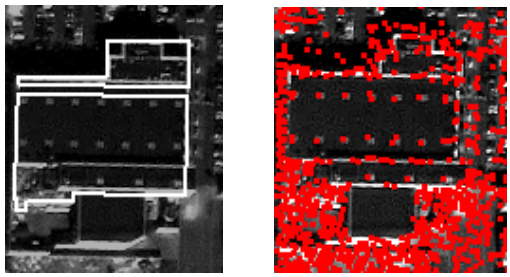

(a) intrusion of building shape

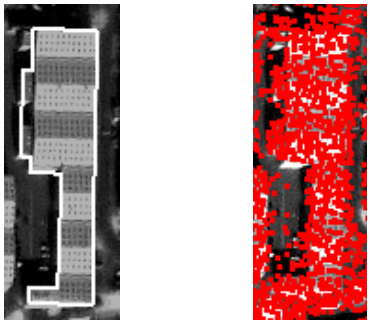

(b) extrusion of building shape

Figure 8. Building extraction errors caused by low point density and building outliers (white line represents building boundaries and red dot represents LIDAR points).

However, our technique suffers several difficulties; firstly, "significant" parts of building shape are sometimes recognized as the "open" polygon and removed by the aforementioned heuristic polygon filtering. Thus, the reconstructed building shapes are intruded with some extent from real geometry or split into two separate objects (see Figure 8 (a)). This problem occurs when LIDAR points are located over the building roof with extremely low density, by which "empty" polygons are generated inside the building outline by recursive BSP. This error could be avoided if LIDAR data with higher density is used or LIDAR data is evenly distributed so that parameters used for the heuristic filter can be regularized. Secondly, we can observe the reverse case of the former problem, in which some building boundaries are extruded from original features (see Figure 8 (b)). This problem is caused by two factors. On the one hand, a portion of building-label points is located outside buildings due to planimetric errors embedded into Ikonos Precision product and LIDAR data used. On the other hand, there is a significant deficiency of on-terrain points nearby buildings, particularly in our case. In general, when the both factors are coherently combined with each other, erroneous "closed" polygons are generated, which could be recognized as the "building" polygon. Since on-terrain points are used as an important evidence to verify the "building" polygon, this verification error can be avoided if the on-terrain point is located nearby buildings with higher density.

Considering the mentioned problematic situations and the low density of LIDAR data used, several parameters used for our building extraction technique are carefully selected. The definition of an ignorable building part is given by l_{th} and a_{th}, i.e., 3 metre and 50 square metre respectively. For the heuristic polygon filtering process, an "open" polygon is verified as a building part if building-label points are located with ρ_{th} larger than 0.6. For removing erroneous "closed" polygons, γ and n_{th} are selected as 0.6 and 5 respectively. The expected point spacing d_{th} can be simply computed by the size of underlying polygon and the average point spacing of entire LIDAR data used. Although relatively large number of parameters is required in current implementation, these parameters are intuitive and their selection can be more stabilized if evenly distributed LIDAR data with higher density is used.

Figure 9. Final building extraction result

5. CONCLUSIONS AND FUTURE WORK

In this paper, the reduction of scene complexity in urban area was achieved by a hierarchical segmentation of LIDAR DEM combined with colour information. For the boundary representation of polyhedral building shape, it is assumed "significant" parts of building shape can be reconstructed by the aggregation of convex polygons. This polygonal part segmentation is implemented by Binary Space Partitioning (BSP), in which hyperlines are extracted from Ikonos image and LIDAR space in coherent collaboration of two different data sources. Since our building extraction technique is implemented based upon global-to-fine strategy, it can be thought to be an efficient method dealing with the level-of-detail problem and resulted errors become to be smaller. However, our technique suffers difficulties when the LIDAR data with low density is not evenly distributed. The selection of relatively large number of parameters is not automated and subjective to properties of LIDAR data used. Therefore, future research will be directed towards stabilizing the selection of those parameters with higher density LIDAR data and it will be also useful to extend our technique to 3D reconstruction of roof

structure, in which the polygonal part segmentation of a building roof relies on planar surface attribute.

REFERENCES

Ameri, B. and Fritsch, D., 1999. 3-D reconstruction of polyhedral-like building models. In: *International Archives of Photogrammetry and Remote Sensing*, 32(3-2W5):15-20.

Baillard, C., Schmid, C., Zisserman, A. and Fitzgibbon, A., 1999a. Automatic line matching and 3D reconstruction of buildings from multiple views. In: *International Archives of Photogrammetry and Remote Sensing*, 32(3-2W5):69-80

Baillard, C. and Maitre, H., 1999b. 3-D reconstruction of urban scenes from aerial stereo imagery: a focusing strategy. *Computer Vision and Image Understanding*, 76(3):244-258.

Brunn, A. and Weidner, U., 1997. Extracting buildings from digital surface models. In: *International Archives of Photogrammetry and Remote Sensing*, 32(3-4W2):27-34.

Burns, J.B., Hanson, A.R. and Riseman, E.M., 1986. Extracting straight lines. *IEEE Pattern Analysis and Machine Intelligence*, 8(4): 425-455.

Fischer, A., Kolbe, T. H., Lang, F., Cremers, A. B., Forstner, W., Plumer, L., and Steinhage, V., 1998. Extracting buildings from aerial images using hierarchical aggregation in 2D and 3D. *Computer Vision and Image Understanding*, 72(2):185-203.

Sohn, G. and Dowman, I., 2001. Extraction of buildings from high resolution satellite data. In: Baltsavias, E., Gruen, A., Van Gool, L. (Eds.), *Automated Extraction of Man-Made Objects from Aerial and Space Images (III)*. Balkema Publishers, Lisse, pp.345– 355.

Sohn, G. and Dowman, I.J., 2002. Terrain Surface Reconstruction by the Use of Tetrahedron Model with the MDL Criterion. In: Proceedings of the Photogrammetric Computer Vision, Graz, Austria, September, pp.336-344.

Haala, N., 1994. Detection of building by fusion of range and image data. In: *International Archives of Photogrammetry and Remote Sensing*, 30(3/1):341-346.

Janes, C., Stolle, F., and Collins, R., 1994. Task driven perceptual organization for extraction of rooftop polygons. In: *IEEE Workshop on Applications of Computer Vision*, Sarasota, FL, December, pp.152-159.

Kim, T. and Muller, J.-P., 1995. Using image understanding fusion techniques. In: A. Grün, E.P. Baltsavias & O. Henricsson (eds), *Automatic Extraction of Man-Made Objects from Aerial and Space Images*. Basel: Birkhäuser Velag, pp. 221-230.

Maas, H.-G. and Vosselman, G., 1999. Two Algorithms for Extracting Building Models from Raw Laser Altimetry Data In: *ISPRS Journal of Photogrammetry and Remote Sensing*, 54(23):153-163.

Noronha, S. and Nevatia, R., 1997. Building detection and description from multiple aerial images. In: *Proceedings of IEEE Computer Society Conference on Computer Vision and Pattern Recognition*, Los Alamitos, CA, pp. 588-594.

Schenk, T. and Csatho, B., 2002. Fusion of lidar data and aerial imagery for a more complete surface description. In: *International Archives of Photogrammetry and Remote Sensing*, 34(3A):310-317.

Vosselman, G., 1999. Building reconstruction using planning faces in very high density height data. In: *ISPRS Conference of Automatic Extraction of GIS Objects from Digital Imagery*, Munich, 8-10 September, pp. 87-92.

Vosselman, G. and Suveg, I., 2001. Map based building reconstruction from laser data and images. In: Baltsavias, E., Gruen, A., Van Gool, L. (Eds.), *Automated Extraction of Man-Made Objects from Aerial and Space Images (III)*. Balkema Publishers, Lisse, pp. 231- 242.

Wang, Z. and Schenk, T., 2000. Building extraction and reconstruction from lidar data. In: *International Archives of Photogrammetry and Remote Sensing*, 33(B3):958-964.

Weidner, U. and Förstner, W., 1995. Towards automatic building extraction from high-resolution digital elevation models. *ISPRS Journal of Photogrammetry and Remote Sensing*, 50(4):38-49.

Fuchs, H., Kedem, Z.M. and Naylor, B.F., 1980. On visible surface generation by a priori tree structures. *Computer Graphics*, 14(3): 124-133.